Hindawi
Mathematical Problems in Engineering
Volume 2022, Article ID 8091485, 10 pages
https://doi.org/10.1155/2022/8091485

Research Article

Coevolutionary Framework-Based Constrained Multi-Objective Optimization for Optimal Carbon-Energy Combined Flow of a Power Grid

Feng Pan,[1] Jingming Zhao,[1] Yuyao Yang,[1] Haoyang Feng,[1] Jiahui Cai ,[2] and Tao Yu[2]

[1]*Metrology Center of Guangdong Power Grid Co., Ltd, Qingyuan 511500, China*
[2]*College of Electric Power, South China University of Technology, Guangzhou 510640, China*

Correspondence should be addressed to Jiahui Cai; 20jhcai1@stu.edu.cn

Received 14 March 2022; Revised 30 March 2022; Accepted 1 April 2022; Published 23 April 2022

Academic Editor: Xiao-Shun Zhang

A new constrained multi-objective optimization coevolutionary algorithm (CCMO) based on the NSGA-II algorithm is proposed to cope with the efficient optimization of multiple objectives containing constraints in the optimal combined carbon-energy flow (OCECF). The algorithm improves the convergence of the population by evolving a new auxiliary population that shares effective information with the original population for weak cooperation, offering significant performance advantages. Applying the algorithm for reactive power control on two different-sized IEEE benchmark systems (IEEE-57 and IEEE-300 bus systems), respectively, minimizes carbon emissions and voltage deviations in the grid. Simulation results show that the CCMO algorithm has significant advantages in terms of the convergence speed and Pareto front.

1. Introduction

The emergence of extreme weather and global warming trends has gradually attracted the attention of many scholars, which is closely linked to carbon dioxide (CO_2) emissions. In response to the demand to reduce carbon emissions and mitigate climate change, power operators, as significant producers of CO_2, need to be given prime focus and take action on generation dispatch and grid carbon emissions [1]. In recent years, renewable energy sources such as solar power, wind power, and hydro power have entered the market, but a threatening share of fossil fuel power plants remains. Carbon capture and storage technology is an effectual way to decrease emissions from the power sector's reliance on fossil energy [2]. Economic dispatch plays an influential part in the operation of power systems by searching for the ideal generation mix within the framework of promised units subject to operational safety constraints [3]. Over the past decade, many measures to control carbon emissions have been proposed by researchers and scholars. The widespread integration of wind generation and the expanded use of carbon capture facilities on combustion units can significantly curtail the amount of CO_2 released into the air. Nevertheless, although wind capacity is clean and inexpensive, its volatile nature puts a lot of pressure on the power system dispatch [4]. In order that the carbon emissions can be reduced along with the production costs, a powerful scheduling of an ambient economy through a clean reliable energy for electricity generation with carbon capture was proposed in [5]. With rising attention to climate risk from air pollution and quality issues, inflexibility on the demand side for electricity, and demands for reliability, the power sector is focused on discovering solutions to drive a more productive and greener industry, keep power prices relatively constant, and provide the power generation necessary to meet the future demand while ensuring that the grid meets the resilient needs of local communities [6].

These studies mentioned above mainly focus on the generation side, i.e., the total carbon emissions of the beneficial generators, ignoring the carbon emissions and economic benefits of the grid operators. A composite electric power system of the low carbon-optimized model [7] can properly integrate various objective features such as energy emissions, flame cost, active energy loss, voltage excursion,

and capital loss. This tracking method determines carbon emission obligations but inevitably double-counts carbon emissions [8]. By studying the connection and association between energy use and carbon emissions, the carbon emission flow in the network is proposed and the fundamental computation method of emission is proposed. This problem may be addressed by means of typical optimality techniques, such as affine programming algorithms, Newton's method [9], etc. Nevertheless, the processing suffers from system nonlinearities, function discontinuities, and easy convergence to local minima [10], with unsatisfactory performance. Traditional artificial intelligence algorithms such as genetic algorithms [11] are used to modify them, but due to their low stability of conversion, they can only obtain locally optimal solutions. Particle swarm optimization (PSO) is a swarm intelligence algorithm inspired by the natural behavior of birds [12]. In recent years, the competitive swarm optimizer (CSO) [13] has shown its ability to be competitive in tackling large-scale single-objective optimization problems, and it is a novel swarm algorithm that differs from particle swarm optimization (PSO).

In order to keep a tradeoff between minimizing goals and meeting restraints, several investigators have put together multiple mechanisms for dealing with restraints, which in turn could be classified into two categories, consisting of using separate restraint treatment schemes at separate stages of evolution or in separate subtopics. For instance, the adaptive tradeoff model (ATM) [14] makes use of both distinct types of restrictive limit mechanisms at various stages of evolution, including a polyobjective method and self-adapting punishment factors. The push-pull search (PPS) framework separates the process of searches as a push phase and a pull phase. In the push phase, the population evolves without considering any restrictions, while in the pull phase, all restrictions and goals are considered. NSGA-II [15] has embedded viability within the Pareto domination, in which the viable option governs the unviable option, and the option with fewer infractions of restrictions governs the other option with more infractions of restrictions. The algorithm proposed in this paper applies the search advantages of NSGA-II, evolves an auxiliary population based on the original population, and performs a weak cooperation, which greatly improves the search efficiency by expanding the scope of the search while reducing the search speed.

2. Mathematical Modeling of OCECF

2.1. Carbon-Energy Combined-Flow. In today's available research field, the equilibrium calculation of carbon footprint is generally translated and measured in terms of primary energy consumption, which does not exhibit the specific characteristics of carbon emissions in the power system. As one of the industries with the most significant carbon emissions, the power sector bears the brunt of the responsibility for carbon emissions. Power system carbon streams measure carbon emissions in terms of power system tide calculations. The power system carbon current is a sort of virtual grid flows that rely on power trend calculations to represent the amount of carbon emitted to maintain any path in the power network [9]. For carbon flow, not only factors such as grid configuration, generators' export, and nodal demand affect the fluctuation, but also the carbon intensities of the generators and the joint liability between the power producers and those who use energy. The calculation of CO_2 flows relies mainly on power tides for the purposes of analysis, and the carbon emissions of the entire power system are considered as the CO_2 emissions of the C_P on the generation side. Therefore, it can be described as an accumulation of grid losses C_{loss} and demand-side carbon emissions C_d, as outlined below:

$$C_P = \sum_{w \in W} P_w \delta_w = C_d + C_{\text{loss}}, \tag{1}$$

where P_w in the matrix stands for the power transmission of the w th generator; δ_w refers to the emission intensity of the carbon of the wth generator; and W denotes gensets in total.

Essentially, electricity manufacturers, i.e., power plants as well as electricity grid firms, are principally involved in the quantum and fleet of their own carbon impacts [6]. For factories and ordinary citizens, they are interested in the quantities of their own carbon output. Accordingly, only the former two would unavoidably contribute to multiply calculations of carbon impacts. To refine this matter, the co-responsibility algorithm applies an appropriate disaggregation of the whole carbon impacts of electricity consumers and producers, as summarized below:

$$C_p = \left(1 - \alpha_p\right) C_e + \alpha_p C_{\text{loss}} + \left(1 - \beta_C\right) \alpha_p C_L + \alpha_p \beta_C C_L, \tag{2}$$

where α_P indicates the proportion of producer's duties ($0 < \alpha_P < 1$), which implies that not only the production of energy is held responsible for the entire carbon bill and β_C indicates the proportion of the consumer's role, $0 < \beta_C < 1$.

The grid company is obligated for the carbon footprint with respect to carbon flows by performing an analysis of the active power damage through the power tidal network. The power losses can be characterized as shown below:

$$P_{\text{loss}} = \sum_{i,j \in N_L} g_{ij} \left[V_i^2 + V_j^2 - 2 V_i V_j \cos \theta_{ij} \right], \tag{3}$$

where V_i and V_j represent the amount of voltage of the ith and jth nodes; g_{ij} shows the conductivity of line i-j; θ_{ij} means the variation of the voltage phasor angle (node i and j); and N_L shows the branch set.

As such, the grid company performs the corresponding liability of capital reduction C_{pgc}, which could be counted accordingly as follows:

$$C_{\text{pgc}} = \alpha_p C_{\text{loss}} + \left(1 - \beta_C\right) \alpha_p C_L, \tag{4}$$

where C_{loss} is derived by performing calculations based on proportional allocation, and the proportionate contribution rules can be displayed as listed below:

$$C_{ds} = \sum_{i,j \in N_L} \sum_{w \in W} \left(\frac{\alpha_{jw}^{(-1)} \Delta P_{ij}}{P_j'} \right) P_w \delta_w, \tag{5}$$

where $a_{jw}{}^{(-1)}$ describes the energy power factor between the jth node and wth generator and P_{ij} and P_j' denote the active

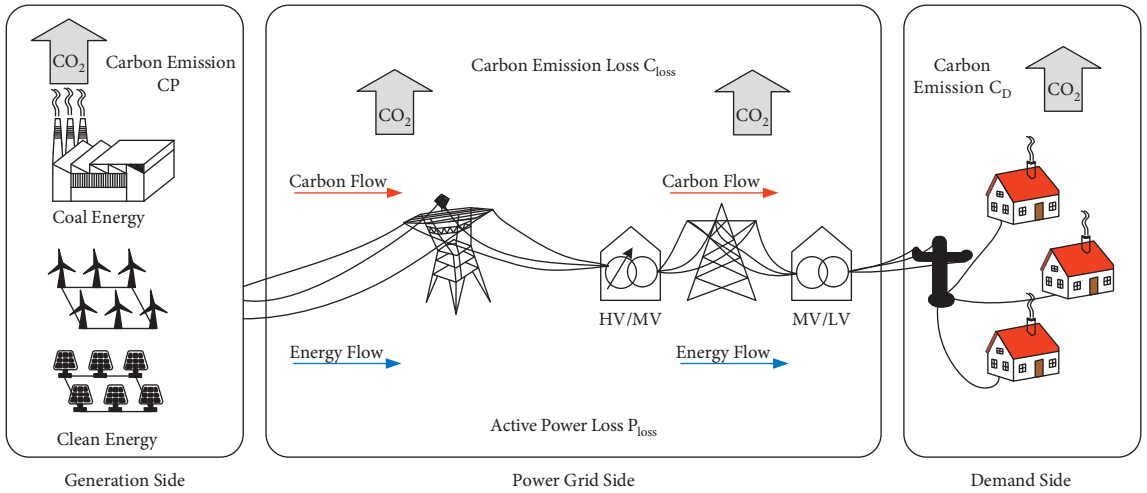

Figure 1: Carbon-energy combined flow of the power grid.

energy depletion of line *i-j* and the aggregate energy stream at the *j*th node in the equivalence of lossless power networks, separately.

2.2. Optimization Model. Active and reactive power dispatch plays a crucial impact on the mixed flow of carbon energy. The power plant, the grid, and the electricity consumers act together and change the active power dispatch scheme; only the grid company influences and acts on the reactive power dispatch. A simplified diagram of the combined carbon-energy flow of the grid is presented in Figure 1. Hence, the OCECF model attempts to minimize the voltage deviation f_1 and minimize the total carbon emission loss f_2. These two objectives need to be accomplished simultaneously and can be written as follows:

$$\begin{cases} \min f_1(x) = V_d, \\ \min f_2(x) = C_{\text{pgc}}. \end{cases} \tag{6}$$

subject to

$$\begin{cases} P_{Gi} - P_{Di} - V_i \sum_{j \in N_i} V_j \left(g_{ij} \cos \theta_{ij} + b_{ij} \sin \theta_{ij} \right) = 0, \\ Q_{Gi} - Q_{Di} - V_i \sum_{j \in N_i} V_j \left(g_{ij} \cos \theta_{ij} - b_{ij} \sin \theta_{ij} \right) = 0, \\ Q_{Gi}^{\min} \le Q_{Gi} \le Q_{Gi}^{\max}, \quad i \in N_G, \\ V_{Ci}^{\min} \le V_i \le V_{Ci}^{\max}, \quad i \in N_i, \\ Q_{Ci}^{\min} \le Q_{Ci} \le Q_{Ci}^{\max}, \quad i \in N_C, \\ T_k^{\min} \le T_k \le T_k^{\max}, \quad k \in N_T, \\ |S_l| \le S_l^{\max}, \quad l \in N_L, \end{cases} \tag{7}$$

where x denotes the subsystem vector, which can be replaced by the voltage at the generator terminals, the individual tap positions of the on-load tap-changer (OLTC) transformer, the total number of connected capacitors and inductors, etc. and V_d represents the voltage deviation index.

The active and reactive power of the *i*th node is expressed by P_{Gi} and Q_{Gi}, respectively; while the active and reactive power demand of the *i*th node is expressed by P_{Di} and Q_{Di}, respectively. Q_{Ci} is the reactive power compensation of the *i*th node; B_{ij} is the sensitivity rate of transmission lines *i-j*; T_k is the transformer tap ratio; S_l is the apparent power of transmission line *l*; N_i is the node set; N_G is the unit set; N_C denotes the device group used to compensate the reactive power; N_T is the set of transformer taps; and N_L is the group of branches. In turn, the index of voltage deviation is specified as follows: [8]

$$V_d = \sum_{i \in N_i} \left\| \frac{2V_i - V_i^{\max} - V_i^{\min}}{V_i^{\max} - V_i^{\min}} \right\|. \tag{8}$$

3. Coevolutionary Framework for Constrained Multi-Objective Optimization Problems (CCMO) for OCECF

3.1. Optimization Introduction. Constrained multi-objective optimization problems are very common in engineering applications, and multiple objectives as well as multiple constraints are difficult for the algorithms to handle at the same time. Some evolutionary algorithms perform well on most multi-objective optimization problems but perform poorly on convergence or diversity when there are many constraints. To face this dilemma, a coevolutionary framework for constrained multi-objective optimization was developed, which consists of the same optimizer evolving two different populations Population1 and Population2. The former solves the initial optimization problem, and the latter solves the auxiliary problem derived from the evolution of the initial optimization problem, and these two populations share and use each other for useful information. The circulating process flow chart of the proposed CCMO is presented in Figure 2.

The sequence of the operation of the algorithm is illustrated in depth as follows:

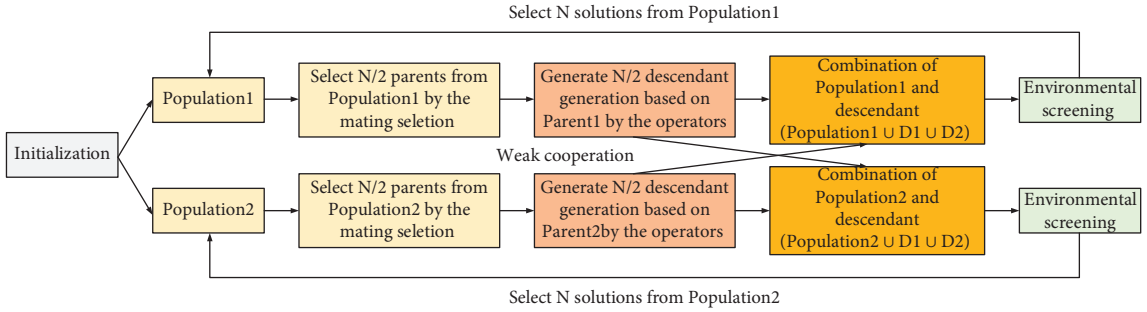

Figure 2: Circulating process flow chart of the proposed CCMO.

(1) Initialization:The presented algorithm begins by randomly generating two initial population Population1 and Population2 whose population size is N.

(2) Screening evolutionary process: In per round of iterations, two parent sets Parent1 and Parent2 are chosen from Population1 and Population2, respectively, using either of the mating selection strategies in the multi-objective optimization algorithm.

(3) Evolutionary process of mating: The above-mentioned two parent sets (Parent1 and Parent2) were crossed separately to produce one descendant population each, i.e., the process yielded two descendant populations. Then, Population1 and Population2 are combined with the two descendant populations by mating, and the newly generated populations are further screened for evolution through a strategy of environmental screening.

(4) Output: The optimal result of the final iteration is returned to the Population1.

3.2. Case Studies of CCMO for OCECF

3.2.1. Introduction and the Computational Complexity. OCECF is controlled on the principle of reactive power dispatching; hence, generator terminal voltage, transformer tap ratio, and reactive power compensation of shunt capacitors act as controllable variables in this paper. The algorithm uses NSGA-II as a co-optimizer for the evolution of the two populations. Assuming that N serves as the density of stock size, D serves as the set of decision variables, M serves as the number of objectives, and the least-case time complexity of mating selection, genetic operator, and selection on the setting for NSGA-II is $O(N)$, $O(ND)$, and $O(MN^2)$, respectively.

CCMO evolved both populations under the same strategy (NSGA-II), so the least-case time complexity of mating selection, inheritance operators, and selection on the environment for CCMO is as follows

$$\begin{aligned} 2 \times O\left(N^2\right) &= O(N), \\ 2 \times O\left(\frac{N}{2} D\right) &= O(ND), \\ 2 \times O\left(MN^2\right) &= O\left(MN^2\right). \end{aligned} \tag{9}$$

Table 1: Main parameters of CCMO and PPS.

Algorithm	Parameters setting	IEEE-57	IEEE-300
CCMO	The number of populations N	50	100
	The maximum iterations	50	100
	The set of decision variables D	7	7
	The number of objectives M	2	2
PPS	The number of populations N	50	100
	The maximum iterations	50	100
	The set of decision variables D	7	7
	The number of objectives M	2	2
	A	0.95	0.95
	T	0.1	0.1
	Cp	2	2
	L	20	20

The proposed CCMO has the same worst-case time complexity as the used NSGA-II.

3.2.2. Parameter Setting. There are two commonly available power systems (IEEE-57 bus system and IEEE-300 bus system) that have been adopted to serve as benchmark systems. The initial problem in CCMO is set to function (6) in OCECF in the experiments, and the auxiliary problem is set to the primary problem in the absence of any restrictions. Simulated binary crossover [16] and polynomial mutation [17] were used to generate offspring in CCMO, where the former probability was set to 1 and the latter one was set to $1/D$, and the distribution index of crossover and mutation was set to 20. To further enhance population diversity, the truncation strategy in SPEA2 [18] was used in the environmental screening. The number of objectives M is set to 2 (the voltage deviation index V_d and the carbon emission intensity C_{pgc}) and the set of decision variables D is 7. The number of populations N and the maximum number of iterations MaxIteration are set to 150 in the IEEE-57 and set to 100 in the IEEE-300, separately. PPS, a typically applicable algorithm with good convergence, is selected for comparison experiments to compare the convergence and divergence on the model of OCECF. The parameters of the comparison algorithm are kept consistent with the proposed algorithm during the experiments. The main parameters of CCMO and PPS are given in Table 1. Moreover, the flow chart of CCMO-based OCECF is displayed in Figure 3.

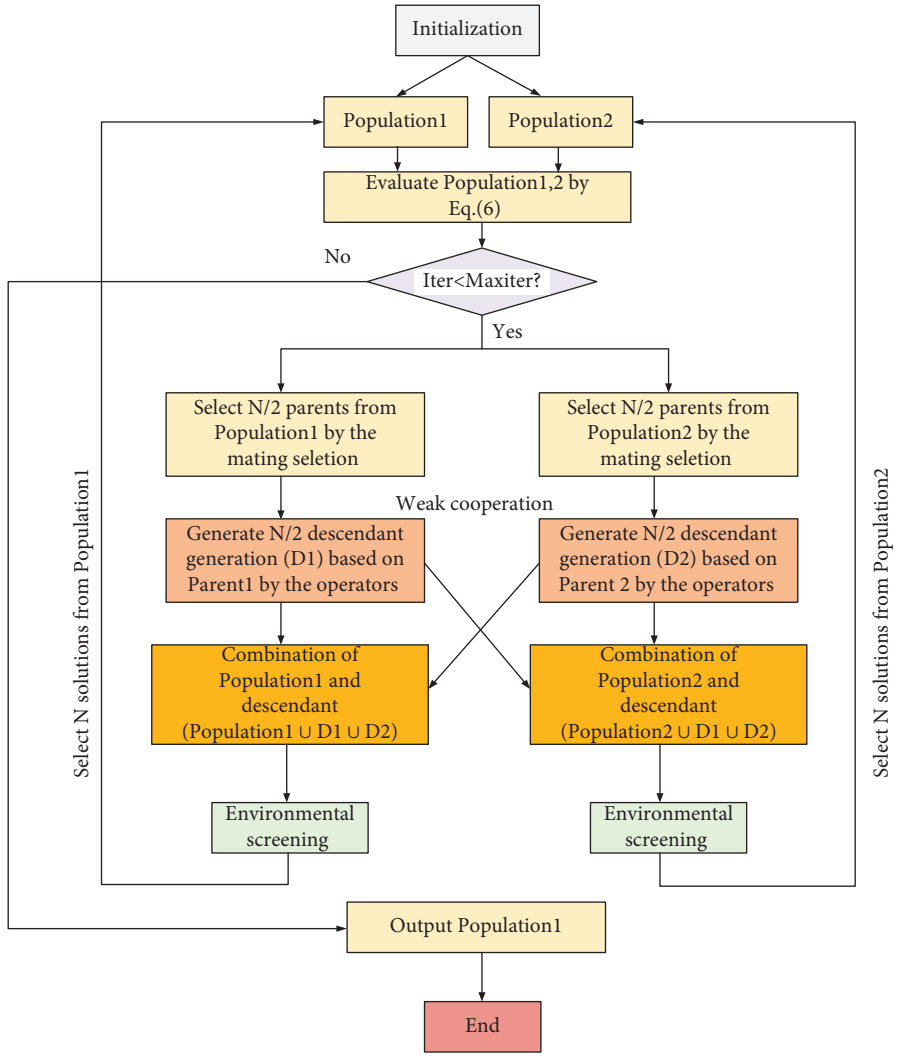

Figure 3: Flow chart of the proposed CCMO for OCECF.

Table 2: Controllable variables of IEEE-57 and IEEE-300 bus systems.

System	Controllable variables	
	Reactive compensation	Transformer tap
IEEE-57	Nodes 18, 25, 53	Circuits 4–18, 21–20, 34–32, 39–57, 7–29, 9–55
IEEE-300	Nodes 117, 120, 154, 164, 166, 173, 190, 231, 238, 240, 248	Circuits 9021–9022, 9002–9024, 9023–9025, 9023–9026, 9007–9071, 9007–9072, 9003–9031, 9003–9032, 9003–9033, 9004–9041, 9004–9042, 9004–9043, 9003–9034, 9003–9035, 9003–9036, 9003–9037, 9003–9038, 213–214, 222-237,227-231, 241–237, 45–46, 73–74, 81–88, 85–99, 86–102, 122–157, 142–175, 145–180, 200–248, 211–212, 223–224, 196–2040, 7003–3, 7061–61, 7166–166, 7024–24, 7001–1, 7130–130, 7011–11, 7023–23, 7049–49, 7139–139, 7012–12

4. Case Studies

The NSGA-II based CCMO model was built due to its wide applicability and good performance on most models. The Pareto front distribution of the OCECF model based on CCMO and the comparison algorithm (PPS) on the IEEE-57 and IEEE-300 systems is shown below, with the same simulation parameter settings in MATLAB for both algorithms. The IEEE-57 system has 7 generators, 57 buses, 80 branches, 17 transformers, 3 reactive power compensation units, and 42 loads. In contrast, the IEEE-300 system has 69 generators, 300 buses, 411 branches, 107 transformers, 29 reactive power compensation devices, and 201 loads. In both IEEE-57 and IEEE-300 bus systems [19], the controllable variables are the combination of reactive power compensation setting gears and transformer taps that minimize the objective function. Table 2 illustrates the controllable variables of the IEEE-57 and IEEE-300 bus systems.

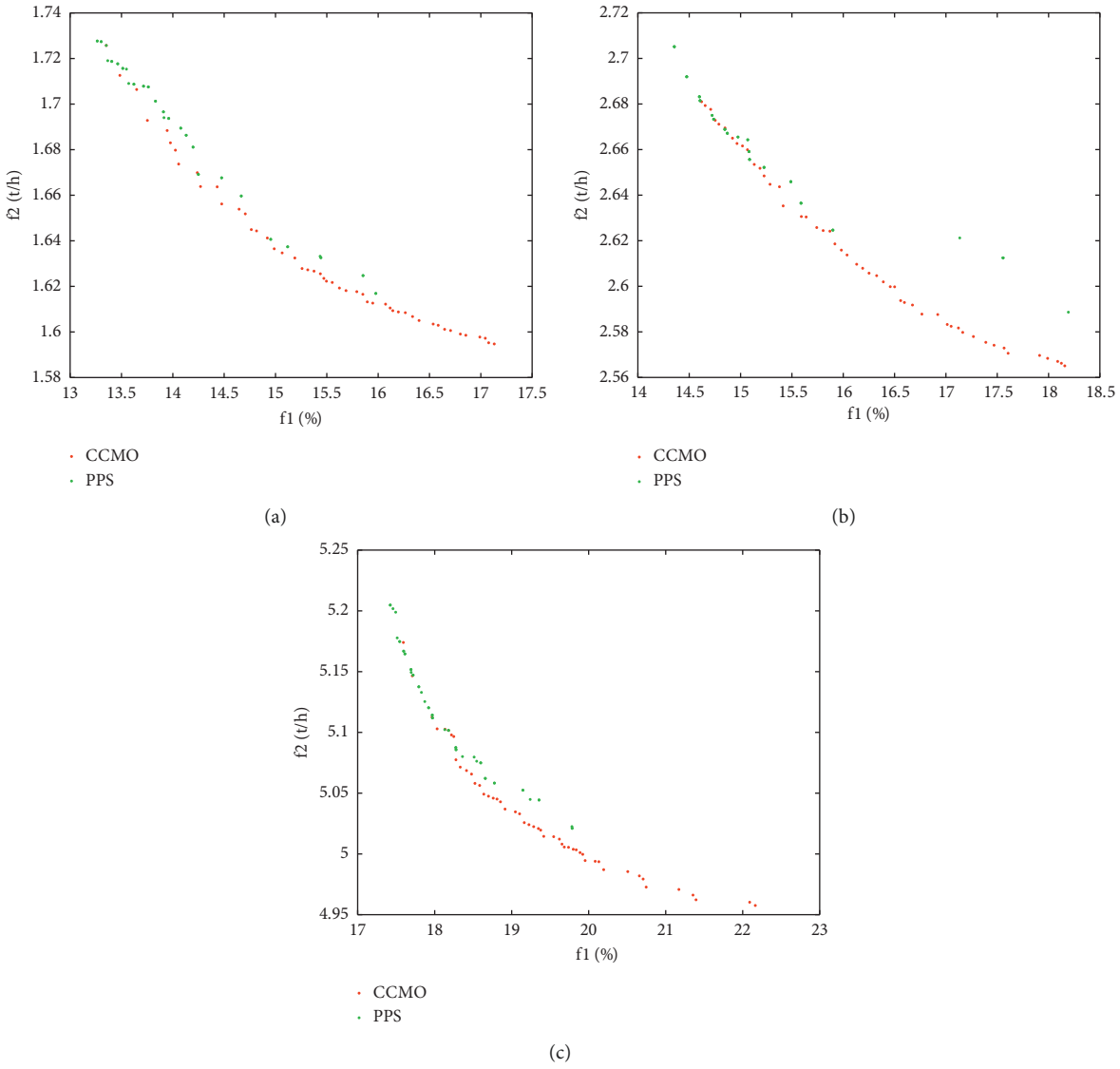

Figure 4: Comparison of OCECF models based on CCMO and PPS at different typical time points on the IEEE-57 system: (a) IEEE-57 at 5 : 00; (b) IEEE-57 at 15 : 00; and (c) IEEE-57 at 20 : 00.

Figures 4(a)–4(c) plot the presentation of algorithms CCMO and PPS applying the OCECF model on a typical small-scale IEEE-57 system. Also, Figures 5(a)–5(c) plot the performance of these two algorithms on an IEEE-300 large-scale system. It can be seen from figures below that the CCMO algorithm is superior to PPS in terms of the degree of convergence of the Pareto solution and the uniformity of the distribution. In the small-scale 57-node system, the advantages of the CCMO algorithm are mainly reflected in its fast computational speed and less solution convergence rate and nondominated solutions. However, in the large-scale 300-node system, the performance of CCMO (including the computational speed, convergence speed, solution value domain, and solution distribution) is more clearly presented in the figure.

Technique for Order Preference by Similarity to Ideal Solution (TOPSIS) is a commonly used multi-objective decision analysis method. It determines the optimal solution or the ranking among solutions by calculating the relative closeness to the positive and negative ideal points (the optimal and inferior solutions of each indicator) and combining the multiple objectives into one value. In this paper, an attempt is made to synthesize the results of the Pareto front using the TOPSIS method, where the distance is calculated using the Euclidean distance, yielding the need to satisfy the minimization of carbon emissions and voltage deviations, making it more suitable for practical applications. Taking a day as an example, one point was taken every 15 minutes, i.e., divided into 96 points. Moreover, the two algorithms mentioned above (CCMO and PPS) were applied on OCECF for one complete day, and the resulting optimal solutions of the Pareto front corresponding to the carbon intensity and voltage deviation were plotted separately, and the images are shown in Figures 6–9.

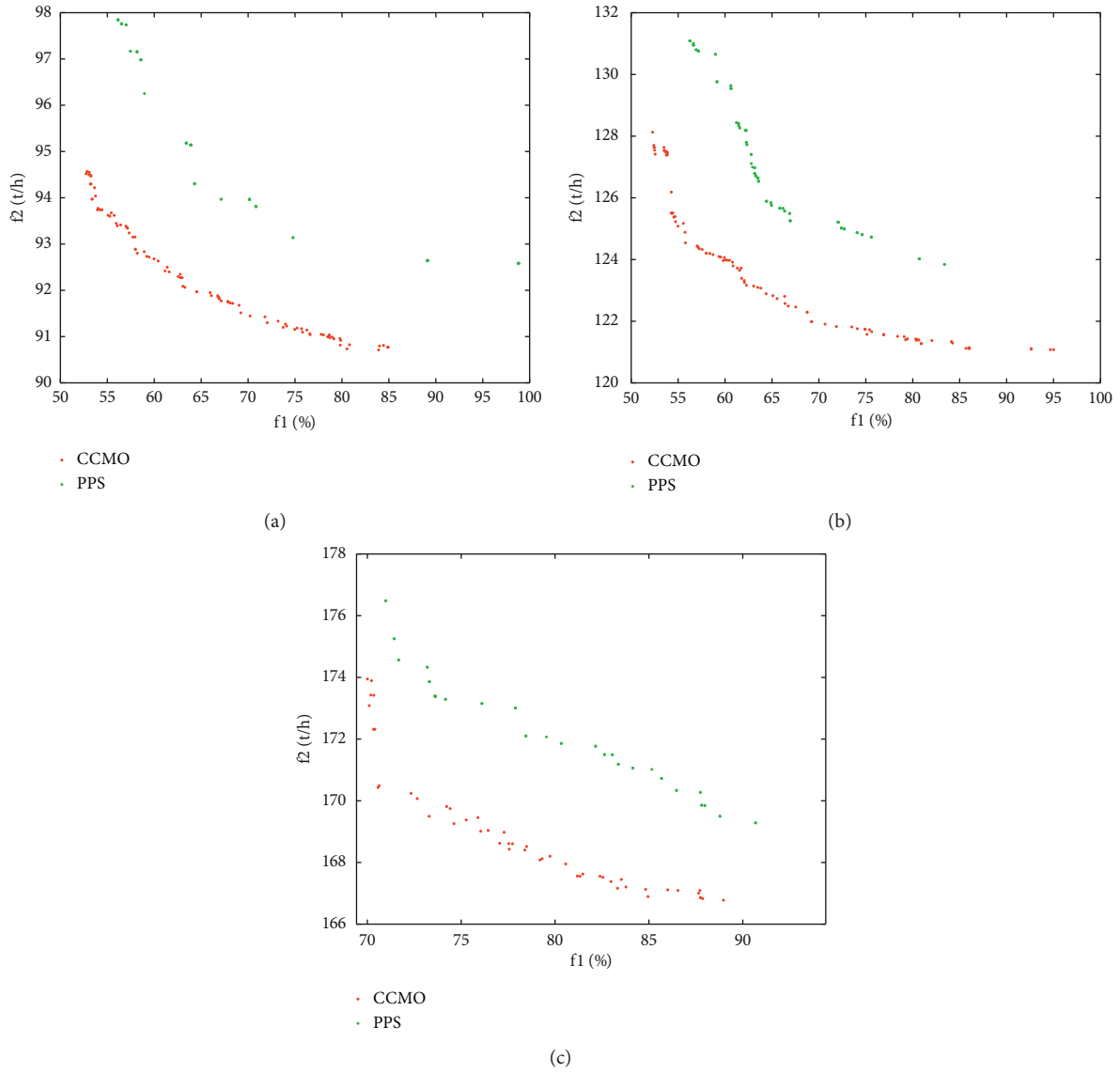

Figure 5: Comparison of OCECF models based on CCMO and PPS at different typical time points on the IEEE-300 system: (a) IEEE-300 at 5 : 00; (b) IEEE-300 at 15 : 00; and (c) IEEE-300 at 20 : 00.

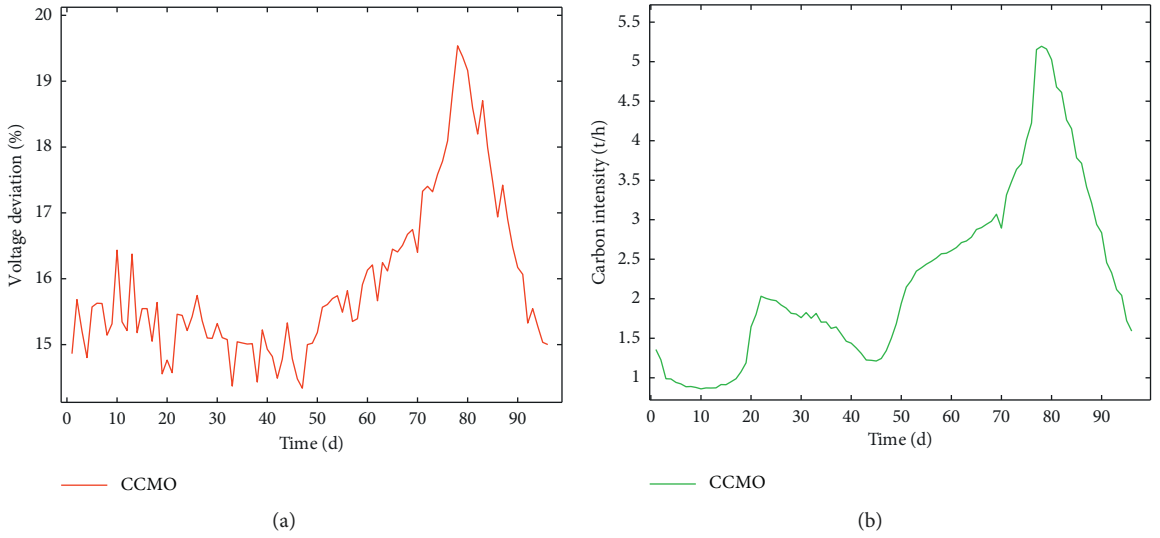

Figure 6: CCMO-based OCECF model on the IEEE-57 system in one day: (a) voltage deviation and (b) carbon intensity.

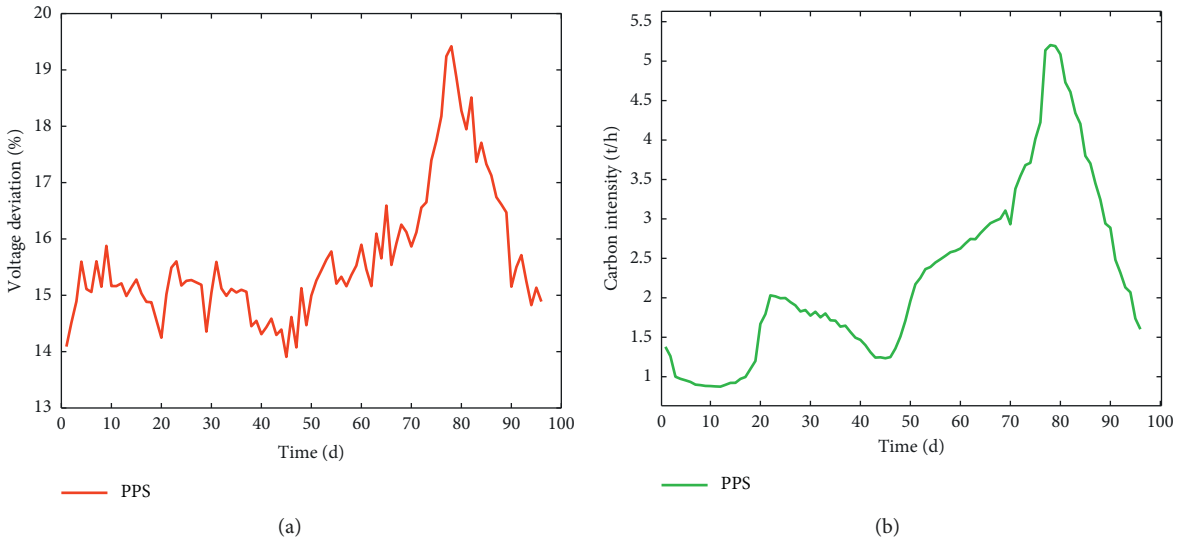

Figure 7: PPS-based OCECF model on the IEEE-57 system in one day: (a) voltage deviation and (b) carbon intensity.

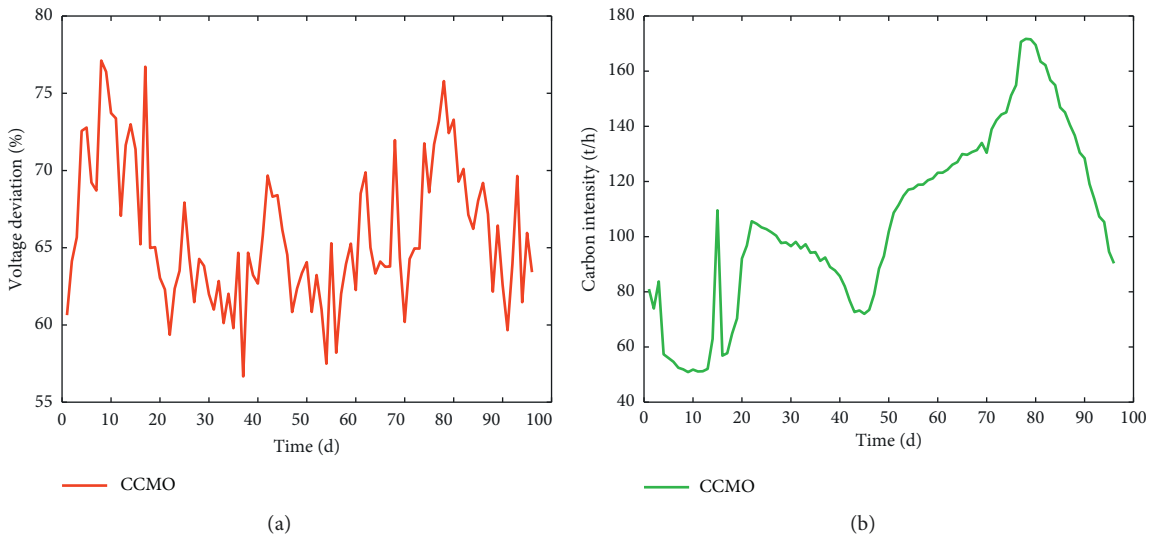

Figure 8: CCMO-based OCECF model on the IEEE-300 system in one day: (a) voltage deviation and (b) carbon intensity.

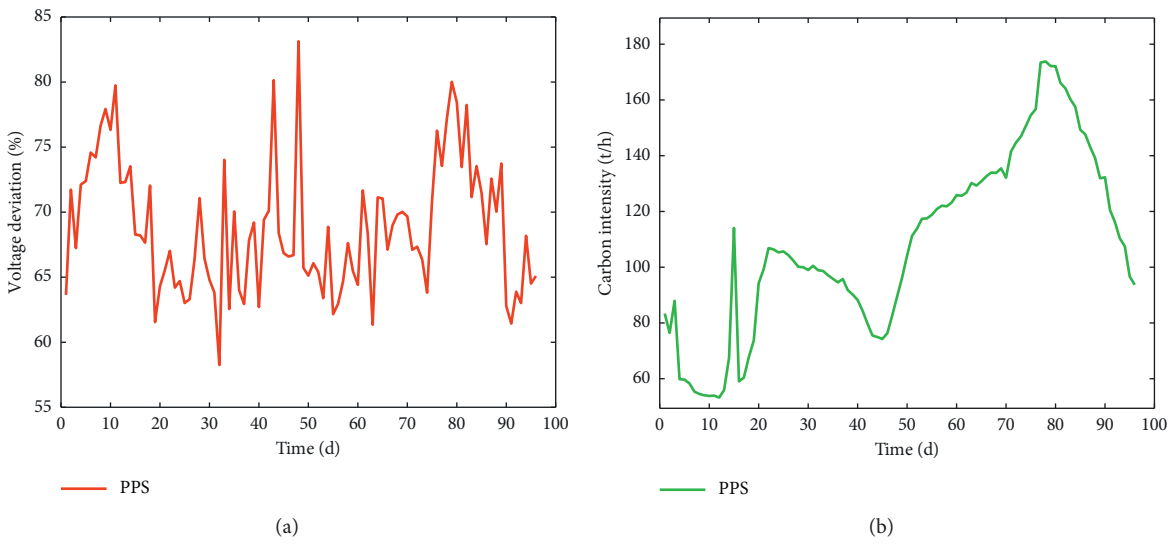

Figure 9: PPS-based OCECF model on the IEEE-300 system in one day: (a) voltage deviation and (b) carbon intensity.

Table 3: Performance results of different algorithms for the IEEE-57 system and IEEE-300 system running for different time periods.

System	Scenario time	PPS			CCMO		
		Convergence time (s)	C_{pgc} (t/h)	V_d (%)	Convergence time (s)	C_{pgc} (t/h)	V_d (%)
IEEE-57	5 : 00	15.99	1.7177	13.4633	14.27	1.7103	15.9080
	15 : 00	14.91	2.7052	16.4138	14.03	2.6242	16.1330
	20 : 00	15.48	5.2275	19.6972	14.20	5.0081	19.6532
IEEE-300	5 : 00	251.54	97.8441	58.7603	203.09	91.6637	57.7965
	15 : 00	234.04	128.7052	63.9092	221.32	125.4731	61.3269
	20 : 00	255.52	174.4435	67.5793	201.40	168.7687	67.3595

As can be seen from Table 3 and Figures 7–9, the CCMO-based OCECF model shows better performance than the PPS on the IEEE-57 and IEEE-300, including less carbon intensity and less voltage deviation. At the same time, it is CCMO that has the superior advantage in terms of calculation speed.

5. Conclusions

This paper develops an OCECF model based on the CCMO co-evolutionary framework, in which two populations evolving in CCMO cooperate with each other to solve the OCECF problem of simultaneously reducing carbon emissions and reducing voltage deviations. In contrast to other algorithms, CCMO solves the original multi-objective problem while evolving another auxiliary population to solve the auxiliary problem derived from the original problem. In contrast to other co-evolutionary algorithms, the CCMO co-evolutionary population takes a weakly cooperative approach, cooperating only in the generation of offspring. As verified in Section 3, CCMO has significant performance advantages when processing the OCECF model for experiments on the IEEE-57 system versus the IEEE-300 system: (1) fast computation and low complexity, (2) superior Pareto front, and (3) small final obtained target values (carbon emission losses and voltage deviations).

Data Availability

The simulation data used to support the findings of this study are available from the corresponding author upon request.

Conflicts of Interest

The authors declare that they have no conflicts of interest.

Acknowledgments

The research presented in this paper is supported by the Science and Technology Project of China Southern Power Grid (No. GDKJXM20212099).

References

[1] S. Tan, J. Yang, J. Yan, C. Lee, H. Hashim, and B. Chen, "A holistic low carbon city indicator framework for sustainable development," *Applied Energy*, vol. 185, pp. 1919–1930, 2017.

[2] S. Reddy, L. K. Panwar, B. K. Panigrahi, and R. Kumar, "Modeling of carbon capture technology attributes for unit commitment in emission-constrained environment," *IEEE Transactions on Power Systems*, vol. 32, no. 1, pp. 662–671, 2016.

[3] J. Wang, A. Botterud, R. Bessa et al., "Wind power forecasting uncertainty and unit commitment," *Applied Energy*, vol. 88, no. 11, pp. 4014–4023, 2011.

[4] R. Ramanathan, "Emission constrained economic dispatch," *IEEE Transactions on Power Systems*, vol. 9, no. 4, 1994.

[5] W. Wei, F. Liu, J. Wang, L. Chen, S. Mei, and T. Yuan, "Robust environmental-economic dispatch incorporating wind power generation and carbon capture plants," *Applied Energy*, vol. 183, pp. 674–684, 2016.

[6] O. Lassagne, L. Gosselin, M. Désilets, and M. C. Iliuta, "Techno-economic study of CO2 capture for aluminum primary production for different electrolytic cell ventilation rates," *Chemical Engineering Journal*, vol. 230, pp. 338–350, 2013.

[7] X. Zhang, T. Yu, B. Yang, L. Zheng, and L. Huang, "Approximate ideal multi-objective solution Q(λ) learning for optimal carbon-energy combined-flow in multi-energy power systems," *Energy Conversion and Management*, vol. 106, pp. 543–556, 2015.

[8] C. Kang, T. Zhou, Q. Chen, Q Xu, Q Xia, and Z Ji, "Carbon emission flow in networks," *Scientific Reports*, vol. 2, no. 1, pp. 479–487, 2012.

[9] D. Sun, B. Ashley, B. Brewer, A. Hughes, and W. Tinney, "Optimal power flow by Newton approach," *IEEE Transactions on Power Apparatus and Systems*, vol. PAS-103, no. 10, pp. 2864–2880, 1984.

[10] B. Zhao, C. X. Guo, and Y. J. Cao, "A multiagent-based particle swarm optimization approach for optimal reactive power dispatch," *IEEE Transactions on Power Systems*, vol. 20, no. 2, pp. 1070–1078, 2005.

[11] X. Yuan, P. Wang, Y. Yuan, Y. Huang, and X. Zhang, "A new quantum inspired chaotic artificial bee colony algorithm for optimal power flow problem," *Energy Conversion and Management*, vol. 100, pp. 1–9, 2015.

[12] R. Poli, J. Kennedy, and T. Blackwell, "Particle swarm optimization," *Swarm intelligence*, vol. 1, no. 1, pp. 33–57, 2007.

[13] R. Cheng and Y. Jin, "A competitive swarm optimizer for large scale optimization," *IEEE Transactions on Cybernetics*, vol. 45, no. 2, pp. 191–204, 2014.

[14] Y. Yong Wang, Z. Zixing Cai, Y. Yuren Zhou, and Z. Wei, "An adaptive t model for constrained evolutionary optimization," *IEEE Transactions on Evolutionary Computation*, vol. 12, no. 1, pp. 80–92, 2008.

[15] K. Deb, A. Pratap, S. Agarwal, and T. Meyarivan, "A fast and elitist multiobjective genetic algorithm: nsga," *IEEE*

Transactions on Evolutionary Computation, vol. 6, no. 2, pp. 182–197, 2002.

[16] K. Deb and M. Goyal, "A combined genetic adaptive search (GeneAS) for engineering design," *Computer Science and Informatics*, vol. 26, pp. 30–45, 1996.

[17] K. Deb and R. B. Agrawal, "Simulated binary crossover for continuous search space," *Complex Systems*, vol. 9, no. 2, pp. 115–148, 1995.

[18] E. Zitzler, M. Laumanns, and L. Thiele, "SPEA2: improving the strength Pareto evolutionary algorithm," Tech. Rep. 103, Swiss Federal Inst. Technol. (ETH), Zurich, Switzerland, Comput. Eng. Networks Lab. (TIK), Munich, Germany, 2001.

[19] X. Zhang, Y. Chen, T. Yu, B. Yang, K. Qu, and S. Mao, "Equilibrium-inspired multiagent optimizer with extreme transfer learning for decentralized optimal carbon-energy combined-flow of large-scale power systems," *Applied Energy*, vol. 189, pp. 157–176, 2017.